Journal of Power Sources 224 (2013) 285–289

Contents lists available at SciVerse ScienceDirect

Journal of Power Sources

journal homepage: www.elsevier.com/locate/jpowsour

Short communication

# Water transport and Schröder's Paradox in fuel cell membrane electrode assemblies

Tak Cheung Yau [a,b], Massimiliano Cimenti [c], Xiaotao T. Bi [a,b,*], Jürgen Stumper [c]

[a] Department of Chemical and Biological Engineering, University of British Columbia, 2360 East Mall, Vancouver, BC V6T 1Z3, Canada
[b] Clean Energy Research Centre, University of British Columbia, 2360 East Mall, Vancouver, BC V6T 1Z3, Canada
[c] Automotive Fuel Cell Cooperation Corporation, 9000 Glenlyon Parkway, Burnaby, BC V5J 5J8, Canada

## HIGHLIGHTS

► Water crossover was observed from oversaturated to saturated side of a MEA in a PEM fuel cell under zero current.
► An additional pressure gradient of 0.5 bar showed no significant influence on water crossover rate.
► Implications for the explanation water crossover results in a running fuel cell were discussed.

## ARTICLE INFO

*Article history:*
Received 11 July 2012
Received in revised form
2 October 2012
Accepted 3 October 2012
Available online 11 October 2012

*Keywords:*
PEM fuel cells
Water crossover
Schröder's Paradox
Nafion (R) membranes

## ABSTRACT

In this work water crossover between anode and cathode compartments of a PEM fuel cell was studied. A net water transport from cathode to anode under zero current was observed when the fuel cell was operated with saturated and oversaturated gases on anode and cathode, respectively. An additional pressure gradient of 0.5 bar from anode to cathode showed no significant influence on water crossover rate. The relevance of these observations to Schröder's Paradox as well as implications for the explanation of water crossover results in a running fuel cell are discussed.



## 1. Introduction

The water content of polymer electrolyte membranes (PEMs) is well known to be important to the internal resistance of PEM fuel cells, while the water content is in turn dependent on the environment the membrane is exposed to [1]. A frequently used empirical relationship between the equilibrium water content of Nafion® at 30 °C was derived by Zawodzinski et al. [2], which showed that the water content increased with increasing relative humidity. At equilibrium, the water content in the membrane exposed to liquid water was higher than the water content in the membrane exposed to saturated vapour, despite the fact that liquid water was in thermodynamic equilibrium with saturated vapour [2]. This phenomenon is known as Schröder's Paradox, and has been interpreted in different ways. Using an in-situ balance, Onishi et al. [3] showed that only the thermal history of the membrane but not the water activity (which equals one for saturated vapour and liquid water) was responsible for the amount of water uptake. They attributed the occurrences of Schröder's Paradox reported in the literature to differences in experimental conditions, membrane thermal history and equilibration time. Jeck et al. [4] employed an inverse microscope combined with a confocal Raman spectrometer to measure water contents within Nafion® membranes. They were able to obtain an isotherm of Nafion® water adsorption in liquid water which overlays on the one in water vapour, by adding polyvinylpyrrolidone to decrease liquid water activity.

Vallieres et al. [5] suggested the Schröder's Paradox can be explained by considering the existence of two points of stability leading to different equilibrium water contents in liquid and vapour environments. Choi and Datta [6] derived models assuming that there is an additional capillary pressure between water in the pores of the membrane and the vapour (but not liquid water) outside the membrane. This affects the force balance of the vapour equilibrated

* Corresponding author. Clean Energy Research Centre, University of British Columbia, 2360 East Mall, Vancouver, BC V6T 1Z3, Canada. Tel.: +1 604 822 4408; fax: +1 604 822 6003.
*E-mail address:* xbi@chbe.ubc.ca (X.T. Bi).

0378-7753/$ – see front matter © 2012 Elsevier B.V. All rights reserved.
http://dx.doi.org/10.1016/j.jpowsour.2012.10.006

system, which limits water uptake and hence the Paradox. Weber and Newman [7] added the effect of capillary pressure into transport models. Bass and Freger [8] constructed an isotherm of liquid and vapour water adsorption showing discrepancies across the range of water activities studied and the discrepancies were even larger than those predicted by the Choi and Datta [6] model. Nafion® surface rearrangement is also a possible explanation to the Paradox, which leads to higher resistance in water adsorption when contacting water vapour compared to liquid water [9], which limits water uptake.

Most of the studies mentioned above focused on bare membranes under ex-situ conditions. On the other hand, in a functional PEM fuel cell, the preparation of the membrane electrolyte assemblies (MEAs) inevitably induces thermal stresses and therefore the water adsorption and transport behaviour of the membrane in MEAs could also be affected. The aim of this work is to study the response of water transport across an MEA to saturated and oversaturated (i.e. 2-phase liquid water/gas mixture) vapour in an actual fuel cell environment. In addition, interpretation of water crossover data from a running fuel cell in relation to the paradox would also be included.

## 2. Experimental

A single cell with a MEA prepared using in-house standard procedures was tested. The MEA consisted of a catalyst coated Nafion® NRE 211 membrane sandwiched between two Toray GDLs. The assembly was hot pressed over the glass transition temperature of the membrane in order to bond the components together. The active area of the MEA was 50 $cm^2$. The MEA was then put into the cell and conditioned by passing through saturated hydrogen and air streams (at 100% relative humidity, RH) in the anode and cathode channels respectively for 12 h at 60 °C and 2.3 bara.

All experiments were carried out at 60 °C. For the sake of comparison, we define the 'RH' of an oversaturated two-phase flow of water in a dry gas stream to be >100%, as in equation (1), which is also applicable to under-saturated and saturated streams with RH ≤ 100%.

$$\mathrm{RH} = \frac{\dot{n}_{H_2O}}{\dot{n}_{H_2O,sat}} \tag{1}$$

During the experiments, a saturated hydrogen stream (with a RH of 100%) was passed through the anode channels while the relative humidity of the air stream in the cathode channels varied from 0% to 300%. The flow rates of both streams were $1.49 \times 10^{-3}$ mol $s^{-1}$ on a dry basis. No current was drawn in these experiments so the effects of water and heat generation were eliminated. The water crossover between anode and cathode through the membrane was measured using the set-up described in previous publications [10]. The outlet streams at the anode were diluted to vaporize any liquid water prior to water content measurement by an infrared sensor (Fig. 1a). The sensor was calibrated against the same pump humidifying the streams right before each steady state measurement (Fig. 1b). The reading at the infrared sensor was steady after 10 min. Steady state readings from the flowmeters and infrared sensor was averaged across a 15 min time span to calculate the dry gas flow $\dot{n}_{MFM,cal,A}$ and infrared reading $y_{H_2O,cal,A}$ during calibration; while a 50 min averaging was used to yield gas flows $\dot{n}_{MFM,A}$ and $\dot{n}_{MFC,A}$ and infrared reading $y_{H_2O,out,A}$ during experimentation. The water crossover rate $\dot{n}_{H_2O,X,A}$ and the corresponding overall water crossover flux $\bar{J}_{H_2O,X}$ over an area $A$ were further calculated using a mass balance:

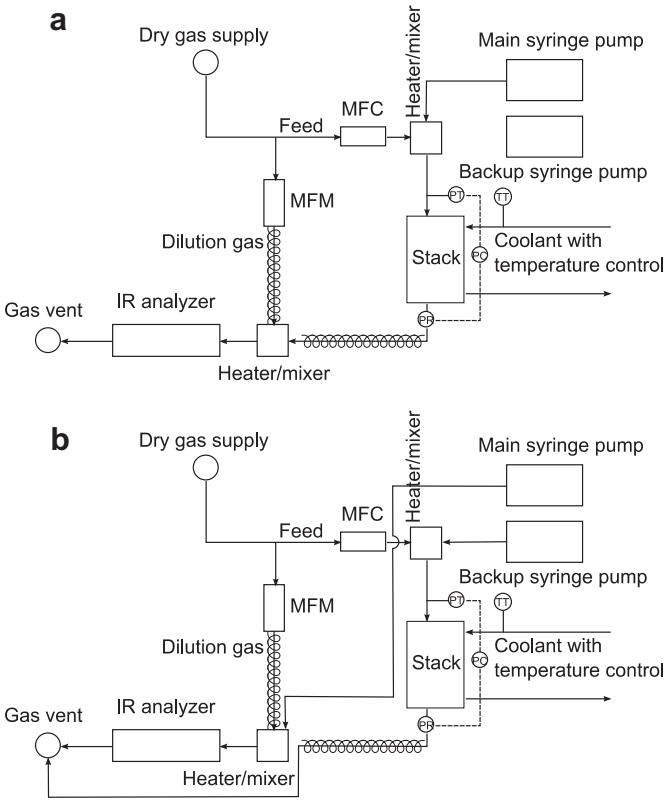


**Fig. 1.** Schematic diagram of the experimental setup. One side/electrode of the setup is shown. (a) Configuration for 'normal mode' measurements, when the water crossover rate for the fuel cell is measured. (b) Configuration for the 'calibration mode', when liquid water from the main syringe pump is fed directly to mix with the dilution gas from MFM and then analyzed by the infrared analyzer as a reference reading, while the backup pump provides humidified flow to maintain steady conditions at the cell. The outlet gases from the cell are purged to the vent. Reprinted from Journal of Power Sources, 196, pp. 9437–9444, Copyright (2011) with permission from Elsevier.

$$\dot{n}_{H_2O,X,A} = \dot{n}_{H_2O,in,A} - \dot{n}_{H_2O,cal,A}\frac{y_{H_2O,out,A}}{y_{H_2O,cal,A}}\left(\frac{\dot{n}_{MFM,A} + \dot{n}_{MFC,A}}{\dot{n}_{MFM,cal,A}}\right) \tag{2}$$

$$\bar{J}_{H_2O,X} = \frac{\dot{n}_{H_2O,X,A}}{A} \tag{3}$$

We define water crossover to be positive from the anode channel to the cathode channel as the convention used in this article. A negative value of water crossover indicates water flows from the cathode channels to the anode channels and a positive value shows water flows from anode channels to cathode channels.

## 3. Results and discussion

Fig. 2 shows the water crossover fluxes from anode to cathode while the cathode inlet RH is varied. The anode inlet RH is 100% for all data points. The pressure at both sides is kept the same at 2.3 bara. When the cathode RH is less than 100% the water crossover flux is positive, meaning water is transported from anode to cathode which can be easily explained by the presence of a water vapour concentration gradient. For oversaturated cathode feeds, the water crossover rate ranges from $-2.4 \times 10^{-7}$ to $-3.6 \times 10^{-7}$ mol $cm^{-2}$ $s^{-1}$. Water is transported from the cathode to anode. The possibility of a systematic error by the equipment is

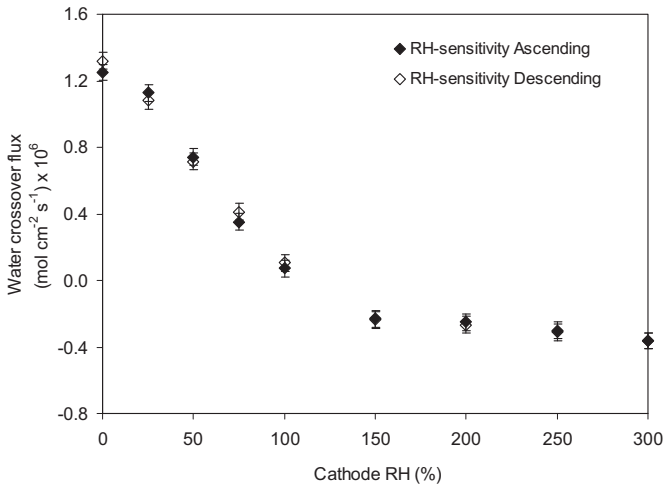


**Fig. 2.** Water crossover flux through the MEA at zero current density. Negative values indicate water transfer from cathode back to anode. Solid symbols are results obtained in an ascending cathode RH sweep, hollow symbols are those obtained in a descending cathode RH sweep. $T = 60\ ^{\circ}C$, $P_A = 2.30$ bara, $P_C = 2.30$ bara, $RH_{in,A} = 100\%$, $H_2$ flow rate $= 1.49 \times 10^{-3}$ mol $s^{-1}$, $N_2$ flow rate $= 1.18 \times 10^{-3}$ mol $s^{-1}$, $O_2$ flow rate $= 3.13 \times 10^{-4}$ mol $s^{-1}$. Error bars indicate the pooled standard deviation estimator as described in equation (10).

very small because the inlet and outlet terms in equation (2) are derived from the same humidification pump. The maximum error in water crossover for different MEAs measured by the equipment was reported by Yau et al. [11] as $1.7 \times 10^{-7}$ mol $cm^{-2}$ $s^{-1}$, which would be much smaller than measured water crossover values in this work as the same MEA is used throughout. This is supported by the water crossover flux at 100% RH both on the anode and cathode compartment, which is very close to zero.

The values for oversaturated conditions are also significantly different from the value under saturated conditions (RHa = RHc = 100%) as the corresponding $t$ statistic is 9.53 and 9 degrees of freedom using the pooled variance estimation, which shows that this is not likely resulted from random errors ($P = 1.2 \times 10^{-5}$) (Please refer to the appendix for the statistics calculations). Water is observed to pass through from the oversaturated cathode side to the saturated anode side, indicating that the liquid water present in the cathode channels promotes water transfer towards the anode side. Hydraulic forces are not significant in this experiment, because the pressure on both sides of the membrane is kept the same at 2.3 bara. On the other hand, assuming that water diffusion through the membrane is the dominant transport mechanism, at the anode interface where water is rejected from the membrane, the water content in the membrane $\lambda_A$ has to be greater than the equilibrium water content $\lambda_{eqm,vapour}$ [12,13]. Or, according to Springer et al. [14], the interface water content is in equilibrium with its environment. In either model, the following is guaranteed:

$$(\lambda_A - \lambda_{eqm,vapour}) \geq 0 \tag{4}$$

Similarly, at the cathode interface the membrane water content $\lambda_C$ is no more than the equilibrium water content $\lambda_{eqm,liquid}$ such that adsorption of water occurs:

$$\left(\lambda_{eqm,liquid} - \lambda_C\right) \geq 0 \tag{5}$$

The transport of water within the membrane from the cathode interface to the anode interface implies that

$$(\lambda_C - \lambda_A) > 0 \tag{6}$$

Therefore

$$\left(\lambda_{eqm,liquid} - \lambda_{eqm,vapour}\right) = \left[\left(\lambda_{eqm,liquid} - \lambda_C\right) + (\lambda_C - \lambda_A) + (\lambda_A - \lambda_{eqm,vapour})\right] > 0 \tag{7}$$

which is the mathematical form of Schröder's Paradox in the membrane.

In Fig. 2 the effect of membrane humidification history on water transport is also illustrated. The solid symbols represent data from an experiment with ascending cathode RH, while hollow symbols represent data from the descending RH experiment which follows immediately after the ascending run. In principle, if the humidification history of the membrane imposes a long term effect on water transfer, there should be some degree of hysteresis with more water transported to the anode side during descending RH experiments. However, by carrying out a paired $t$ test, no statistically significant difference is found between the two sets of corresponding ascending and descending water crossover data ($t$ statistic = 0.505, degree of freedom = 17, $P = 0.620$). This shows that the above results are not an artefact caused by how the membrane is hydrated and hence the consistency of the results.

It should be noted that the magnitudes of the water transfer fluxes at oversaturated test conditions are smaller than the fluxes obtained with a cathode RH of 75% or lower. On the contrary, Adachi et al. (2009) found that when the membrane was exposed to liquid water on one side and water vapour on the other, the crossover flux was a few times higher than that obtained with water vapour on both sides of the membrane. A possible explanation to our findings is as follows. The GDL is hydrophobic, so little liquid water in the oversaturated cathode channels can reach the membrane interface. Therefore only a small part of the membrane experiences a higher flux caused by the Schröder's Paradox; while the other parts have virtually no water crossover under a zero RH gradient. It is reminded that the overall water crossover flux reported in Fig. 2 is averaged all over the area of the membrane and hence a relatively small overall flux is observed. More investigations are required to find out the cause of such results.

The effect of total gas pressure on water transport between saturated and oversaturated channels is illustrated in Fig. 3. No significant difference in water crossover flux is observed for oversaturated feeds even when the anode pressure is reduced from 2.3 bara to 1.8 bara as suggested by a paired $t$ test ($t$ value = 0.015, degree of freedom = 9, $P = 0.988$). No additional water is driven from the cathode to the anode even under a pressure difference of 0.5 bar across the membrane. The additional capillary pressure $P_{cap}$ brought by the condensed water in the pores at the membrane–vapour interface can be calculated by the following equation in Choi and Datta (2003) [6]

$$P_{cap} = (S\sigma\cos\theta) \times \left(1 + \frac{V_{mem}}{V_{H_2O}}\frac{1}{\lambda}\right) \tag{8}$$

where $V_{mem}$ and $V_{H_2O}$ are the molar volumes of the membrane and water, respectively. With a contact angle $\theta$ of 98°, surface tension $\sigma$ of 0.0721 N $m^{-1}$, specific pore surface area $S$ of 210 $m^2$ $cm^{-3}$, and water content $\lambda$ of 14 as given by Choi and Datta [6], $P_{cap}$ is estimated to be 66 bar which is enormously high. If this pressure difference of 66 bar is responsible for Schröder's Paradox [6], the pressure difference of 0.5 bar in our experiments is negligible in changing the pressure balance within the pore/vapour interface.

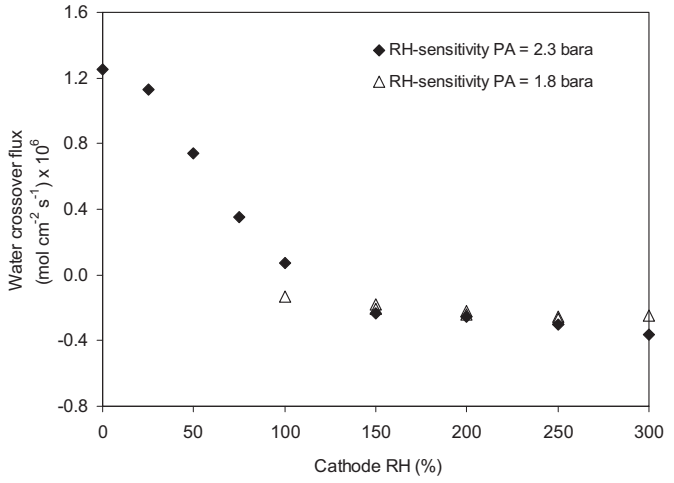


**Fig. 3.** Water crossover flux through the MEA at zero current density. Negative values indicate water transfer from cathode back to anode. Solid symbols are results obtained at $P_A$ = 2.30 bara, hollow symbols are those obtained at $P_A$ = 1.80 bara. $T$ = 60 °C, $P_C$ = 2.30 bara, $RH_{in,A}$ = 100%, $H_2$ flow rate = 1.49 × $10^{-3}$ mol $s^{-1}$, $N_2$ flow rate = 1.18 × $10^{-3}$ mol $s^{-1}$, $O_2$ flow rate = 3.13 × $10^{-4}$ mol $s^{-1}$.

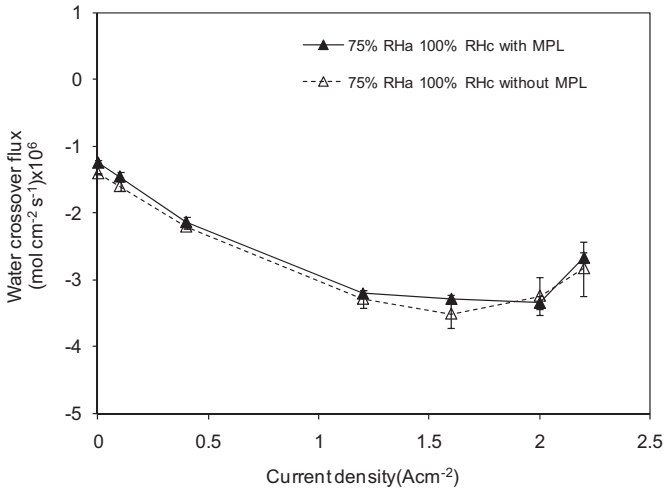


**Fig. 4.** Water crossover flux (measured from anode) against current density. Negative values indicate water transfer from cathode back to anode. Results are the average from two replicates. MEA construction on the cathode side is as indicated. The microporous layer is present in all experiments. $T$ = 70 °C, $P_A$ = 2.30 bara, $P_C$ = 2.30 bara, $RH_{in,A}$ = 75%, $RH_{in,C}$ = 100%, $H_2$ flow rate = 4.46 × $10^{-3}$ mol $s^{-1}$, $N_2$ flow rate = 2.94 × $10^{-3}$ mol $s^{-1}$, $O_2$ flow rate = 7.81 × $10^{-4}$ mol $s^{-1}$. Error bars indicate the difference in readings between the two replicates; solid symbols may cover the whole error bar. Reprinted from Journal of Power Sources, 196, pp. 9437–9444, Copyright (2011) with permission from Elsevier.

Therefore no change in water crossover flux can be observed if the Schröder's Paradox exists.

A possible explanation for our experimental results is that the Nafion® membrane restructures itself when contacting liquid water to become more surface hydrophilic [15]. This can open up more access to the hydrophilic pores in the membrane by better swelling, therefore a higher water content could be achieved at that interface, producing a concentration gradient across the membrane. The ejection of water at the anode interface could be explained by the difference between the membrane water content and the equilibrium water content with saturated vapour at the interface. Extending this argument to an equilibrium situation, it may be deduced that the presence of more accessible channels gives rise to a higher final water content within the membrane, leading to a discrepancy in equilibrium water contents of the membrane in contact with liquid water and saturated vapour.

Schröder's Paradox may also explain the water transport behaviour in operating fuel cells as shown in Fig. 4 [11]. A MEA with a microporous layer on both anode and cathode sides or with a microporous layer on anode side only was subjected to polarization tests along with water crossover measurements. The cathode feed is at 100% RH and the inlet RH at the anode is 75%. More and more water is transported from the cathode side to the anode side when the current density increased from 0 up to a current density of 2 A $cm^{-2}$. At zero current density, the water crossover flux (−1.2 × $10^{-6}$ mol $cm^{-2}$ $s^{-1}$) is much larger in magnitude compared to the corresponding value in Fig. 2 (4 × $10^{-7}$ mol $cm^{-2}$ $s^{-1}$). This may be due to the fact that the anode flow rate (4.46 × $10^{-3}$ mol $s^{-1}$) is larger than the cathode flow rate (3.72 × $10^{-3}$ mol $s^{-1}$) in Fig. 4, while in Fig. 2 the flow rates at both sides are the same at 1.49 × $10^{-3}$ mol $s^{-1}$. This may lead to a draw of water towards the anode side due to convection. The effect of flow rate difference on both sides of the MEA is not considered in this article and may be of interest to be studied in future. Similar results have been reported by Adachi et al. [16] using saturated cathode feed and 40% RH at the anode feed. The effect of hydraulic pressure is not evident, because removing the microporous layer on the cathode side of the membrane does not significantly affect the flow of water across the membrane [11]. The hypothesis of Schröder's Paradox allows water generated by the electrochemical reaction to enter the membrane and transport to the anode side through a concentration gradient, even if the cathode channels are saturated with water vapour. This would be more evident if the anode feed is also saturated and the diffusion gradient across the membrane is zero, as shown in Fig. 7(a) in Kim et al. [17] Both anode and cathode GDLs are identical, and the net water transport coefficient is negative (i.e. water is transported from cathode to anode) while significant electro–osmotic drag is supposed to be present. Secondly, liquid water is more readily absorbed into the membrane compared to water vapour [9,13,16,18]. This also contributes to higher water content at the cathode interface compared to the anode interface which favours back diffusion. In addition, if one considers that the cathode potential loss is translated into heat generation, the membrane is significantly hotter on the cathode side. Water would be dragged towards the colder anode side, which is known as thermo–osmotic drag [19]. All three phenomena listed above can provide insights in explaining the experimental results shown in Fig. 4.

## 4. Conclusions

The transport of water between the anode and cathode sides of a MEA without a current load was measured at different inlet humidification levels and gas pressures. Water was observed to move from an oversaturated cathode stream to a saturated anode stream in the absence of a pressure gradient, which suggests the liquid water present at the cathode created a concentration gradient within the membrane even when the anode stream was saturated, a corollary of the Schröder's Paradox. No hysteresis was observed during RH sweep at the cathode feed. Imposing a lower pressure at the anode side did not enhance the transfer of water because the pressure difference was too small compared to capillary forces. The Paradox, together with lower resistance of liquid adsorption and thermo–osmotic drag, helped to explain the result that in a running fuel cell the membrane could take up the generated water even if the cathode feed was saturated. Further investigations should be carried out in the future to fully understand the phenomenon.

## Appendix A

Assuming equal variance throughout the experiments, a $t$ statistic can be calculated using the following

$$t = \frac{\overline{x}_1 - \overline{x}_2}{s_{x1x2}\sqrt{\frac{1}{n_1} + \frac{1}{n_2}}} \tag{9}$$

with pooled standard deviation

$$s_{x1x2} = \sqrt{\frac{(n_1 - 1)s_{x1}^2 + (n_2 - 1)s_{x2}^2}{n_1 + n_2 - 2}} \tag{10}$$

and $n_1 + n_2 - 2$ degrees of freedom. $\overline{x_1}$ and $s_{x1}$ are the mean and standard deviation of the data with saturated cathode (RHc = 100%) and $n_1 = 2$ samples, $\overline{x_2}$ and $s_{x2}$ are the mean and standard deviation of the data with oversaturated cathode (RHc > 100) and $n_2 = 8$ samples.

For a paired $t$ test with $n_{34}$ pairs of sample $x_3$ and $x_4$, the $t$ statistic is given by

$$t = \frac{\overline{x_3} - \overline{x_4}}{s_{34}\sqrt{n_{34}}} \tag{11}$$

where $s_{34}$ is the standard deviation of the difference between the matching pairs of $x_3$ and $x_4$. The degree of freedom is given by $n_{34}$–1.

## References


[1] F. Barbir, PEM Fuel Cells: Theory and Practice, Academic Press, Amsterdam, 2005.
[2] T. Zawodzinski, C. Derouin, S. Radzinski, R. Sherman, V. Smith, T. Springer, S. Gottesfeld, J. Electrochem. Soc. 140 (1993) 1041–1047.
[3] L.M. Onishi, J.M. Prausnitz, J. Newman, J. Phys. Chem. B 111 (2007) 10166–10173.
[4] S. Jeck, P. Scharfer, M. Kind, J. Membr. Sci. 373 (2011) 74–79.
[5] C. Vallieres, D. Winkelmann, D. Roizard, E. Favre, P. Scharfer, M. Kind, J. Membr. Sci. 278 (2006) 357–364.
[6] P. Choi, R. Datta, J. Electrochem. Soc. 150 (2003) E601–E607.
[7] A. Weber, J. Newman, J. Electrochem. Soc. 151 (2004) A311–A325.
[8] M. Bass, V. Freger, Polymer 49 (2008) 497–506.
[9] T. Romero, W. Mérida, J. Membr. Sci. 338 (2009) 135–144.
[10] P. Sauriol, D. Nobes, X. Bi, J. Stumper, D. Jones, D. Kiel, J. Fuel Cell. Sci. Technol. 6 (2009) 041014.
[11] T.C. Yau, M. Cimenti, X. Bi, J. Stumper, J. Power Sources 196 (2011) 9437–9444.
[12] P. Berg, K. Promislow, J. St Pierre, J. Stumper, B. Wetton, J. Electrochem. Soc. 151 (2004) A341–A353.
[13] S. Ge, X. Li, B. Yi, I. Hsing, J. Electrochem. Soc. 152 (2005) A1149–A1157.
[14] T. Springer, T. Zawodzinski, S. Gottesfeld, J. Electrochem. Soc. 138 (1991) 2334–2342.
[15] S. Goswami, S. Klaus, J. Benziger, Langmuir 24 (2008) 8627–8633.
[16] M. Adachi, T. Navessin, Z. Xie, F. Li, S. Tanaka, S. Holdcroft, J. Membr. Sci. 364 (2010) 183–193.
[17] T. Kim, S. Lee, H. Park, Int. J. Hydrog. Energy 35 (2010) 8631–8643.
[18] M. Adachi, T. Navessin, Z. Xie, B. Frisken, S. Holdcroft, J. Electrochem. Soc. 156 (2009) B782–B790.
[19] W. Dai, H. Wang, X. Yuan, J. Martin, D. Yang, J. Qiao, J. Ma, Int. J. Hydrog. Energy 34 (2009) 9461–9478.